Adaptive Modeling of Ionic Membrane Currents Improves Models of Cardiac Electromechanics

NHL Kuijpers[1], HMM ten Eikelder[2], FW Prinzen[1]

[1]Maastricht University, Maastricht, The Netherlands
[2]Eindhoven University of Technology, Eindhoven, The Netherlands

Abstract

A change in activation sequence by means of pacing induces changes in action potential (AP) morphology and duration. These changes are caused by electrical remodeling of ionic membrane currents and are reflected in the T wave in the electrocardiogram (ECG). Also the calcium transient is affected, which leads to changes in cardiomechanics. By modeling the cardiac muscle as a single fiber, we investigated whether electrical remodeling may be triggered by changes in mechanical load. A homogeneous distribution of electrophysiology in our model resulted in an inhomogeneous distribution of stroke work. After remodeling of the ionic membrane currents, contraction was more homogeneous and the repolarization wave was reversed. These results are in agreement with experimentally observed homogeneity in mechanics and heterogeneity in electrophysiology. In conclusion, adaptive modeling of electrophysiology may improve current models of cardiac electromechanics.

1. Introduction

Regional variation in action potential (AP) duration and morphology is related to regional differences in ionic membrane currents. Transmural heterogeneity in electrophysiology is related to differences in excitation-contraction coupling (ECC) and is believed to help synchronize contraction of the heart muscle [1]. In models of cardiac electromechanics, heterogeneity in electrophysiology and ECC should be incorporated to obtain a more homogeneous mechanical behavior as observed in experiments [2, 3].

In 1982, Rosenbaum *et al.* [4] observed that longer lasting epicardial pacing leads to a change in the T wave of the ECG. With normal sinus rhythm, concordance of the T wave reappears after some time. Since it appears that the cardiac myocytes somehow "remember" their original state, this phenomenon is known as "cardiac memory" [4]. The observed changes in the T wave are related to remodeling of ionic membrane currents. Since electrical remodeling also involves the calcium transient, it is expected that the mechanical behavior of the heart muscle is affected.

Recent experimental observations indicate that electrical remodeling is triggered by changes in mechanical load (mechanoelectric feedback) [5, 6]. In this paper, we hypothesize that electrical remodeling is a way to obtain a more homogeneous contraction of the heart muscle. Based on this hypothesis, we propose an adaptive modeling method in which ionic membrane currents adapt to changes in mechanical load such that a more homogeneous distribution of stroke work is obtained.

2. Methods

Cardiac electrophysiology and mechanics is modeled by the Cellular Bidomain Model [7–9]. The heart muscle is represented as a string of segments that are electrically and mechanically coupled.

2.1. Cardiac electrophysiology

The electrophysiological state of each segment is defined by the intracellular potential (V_{int}), the extracellular potential (V_{ext}), and the state of the cell membrane, which is expressed in gating variables and ion concentrations. The membrane potential (V_{mem}) is defined by $V_{\text{mem}} = V_{\text{int}} - V_{\text{ext}}$. Exchange of current between the intracellular and extracellular domains occurs as transmembrane current (I_{trans}), which depends on ionic current (I_{ion}) and capacitive current according to

$$I_{\text{trans}} = \chi(C_{\text{mem}}\frac{\mathrm{d}V_{\text{mem}}}{\mathrm{d}t} + I_{\text{ion}}), \tag{1}$$

where $\chi = 2000\ \text{cm}^{-1}$ is the ratio of membrane area to tissue volume and $C_{\text{mem}} = 1.0\ \mu\text{F/cm}^2$ represents membrane capacitance per unit membrane surface.

To model I_{ion}, we apply the Courtemanche-Ramirez-Nattel model [10]. The total ionic current is given by

$$\begin{aligned} I_{\text{ion}} \quad = \quad & I_{\text{Na}} + I_{\text{K1}} + I_{\text{to}} + I_{\text{Kur}} + I_{\text{Kr}} + I_{\text{Ks}} + I_{\text{Ca,L}} \\ & + I_{\text{p,Ca}} + I_{\text{NaK}} + I_{\text{NaCa}} + I_{\text{b,Na}} + I_{\text{b,Ca}}, \end{aligned} \tag{2}$$

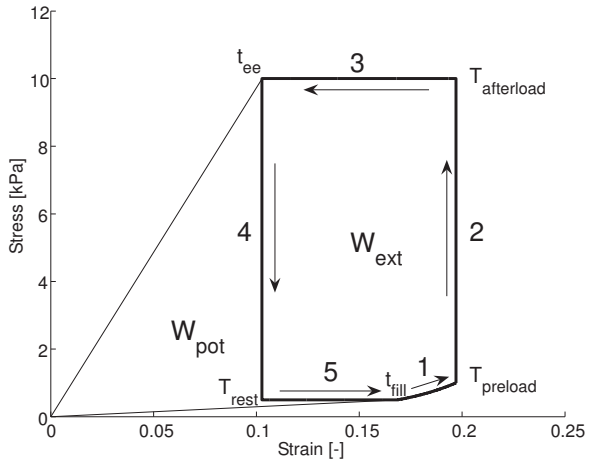

Figure 1. Overview of the cardiac cycle. The numbers indicate the five phases as follows: 1 filling, 2 isovolumic contraction, 3 ejection, 4 isovolumic relaxation, and 5 isotonic relaxation. The arrows indicate the direction of time; t_{fill} indicates the time at which filling starts and t_{ee} the time at end of ejection. A cardiac cycle was simulated with minimum load $T_{\text{rest}} = 0.5$ kPa, preload $T_{\text{preload}} = 1$ kPa, and afterload $T_{\text{afterload}} = 10$ kPa. Strain is defined as $\lambda - 1$, where λ is the stretch ratio. External stroke work density (W_{ext}) is the area indicated by W_{ext} and potential work density (W_{pot}) is the area indicated by W_{pot}. Total stroke work density (W_{tot}) is the sum of W_{ext} and W_{pot}.

where I_{Na} is fast inward Na^+ current, I_{K1} is inward rectifier K^+ current, I_{to} is transient outward K^+ current, I_{Kur} is ultrarapid delayed rectifier K^+ current, I_{Kr} is rapid delayed rectifier K^+ current, I_{Ks} is slow delayed rectifier K^+ current, $I_{\text{Ca,L}}$ is L-type Ca^{2+} current, $I_{\text{p,Ca}}$ is Ca^{2+} pump current, I_{NaK} is Na^+-K^+ pump current, I_{NaCa} is Na^+/Ca^{2+} exchanger current, and $I_{\text{b,Na}}$ and $I_{\text{b,Ca}}$ are background Na^+ and Ca^{2+} currents [10]. The model also describes Ca^{2+} handling by the sarcoplasmic reticulum (SR) and Ca^{2+} buffering mediated by troponin, calmodulin, and calsequestrin [10].

2.2. Cardiac mechanics

The mechanical behavior of a single segment is modeled by a series elastic, a contractile, and a parallel elastic element. In the undeformed state, all segments have the same length (0.1 mm) and cross-sectional area (0.01 mm^2). Active force generated by the contractile element is described by *Model 4* of Rice *et al.* [11] and is related to intracellular Ca^{2+} concentration and sarcomere length [7, 9]. It follows from mechanical equilibrium that the tension generated by each segment must be equal to the tension applied to the fiber.

To simulate the cardiac cycle, we distinguish five phases as indicated in Figure 1. During filling, ejection, and isotonic relaxation, the load applied to the cardiac fiber (T_{fiber}) is set as a boundary condition, whereas during isovolumic contraction and isovolumic relaxation, the stretch ratio of the fiber (λ_{fiber}) is a boundary condition. To initiate contraction, the first segment is electrically stimulated at the beginning of isovolumic contraction.

2.3. Electrical remodeling of $I_{\text{Ca,L}}$

After three weeks of epicardial pacing, Plotnikov *et al.* [12] observed a more positive activation and slower inactivation of $I_{\text{Ca,L}}$ in epicardial myocytes. To incorporate these observations in our model, $I_{\text{Ca,L}}$ kinetics are adapted by shifting the voltage-dependency of the activation gating variable with at most 10 mV. Adaptation of $I_{\text{Ca,L}}$ is represented with parameter ρ, which ranges between -1.0 (-10 mV shift) and 1.0 ($+10$ mV shift). The reference situation is represented by $\rho = 0.0$ (no shift). A positive value of ρ results in a slower decrease of $I_{\text{Ca,L}}$ during the plateau phase of the AP and leads to an increased APD and Ca^{2+} transient. A negative value of ρ results in a faster decrease of $I_{\text{Ca,L}}$ and a decreased APD and Ca^{2+} transient [9].

Based on the assumption that electrical remodeling is triggered by changes in mechanical load, we use stroke work per unit of tissue volume as a feedback signal to determine the remodeling parameter ρ. We distinguish between *external* stroke work density (W_{ext}) and *total* stroke work density (W_{tot}). W_{ext} is defined as the area enclosed by the stress-strain loop during the cardiac cycle and W_{tot} is W_{ext} extended with *potential* stroke work density (W_{pot}) (Figure 1).

For each segment n, the remodeling parameter is denoted by ρ_n. The parameters ρ_n are determined such that stroke work is homogeneously distributed over the fiber. As reference, we use stroke work generated by the segment in the center of a homogeneous fiber ($\rho_n = 0.0$ for all segments). The ρ_n are then found by iteratively computing stroke work for each segment followed by adapting the ρ_n until the ρ_n no longer change. Initially, $\rho_n = 0.0$ for each segment n. Each time a new cardiac cycle starts, ρ_n is adapted by

$$\rho_n \rightarrow \begin{cases} \rho_n + 0.01 & \text{if } W_n < 0.99 \cdot W_{\text{ref}} \text{ and } \rho_n < 1.0 \\ \rho_n - 0.01 & \text{if } W_n > 1.01 \cdot W_{\text{ref}} \text{ and } \rho_n > -1.0 \\ \rho_n & \text{otherwise} \end{cases}$$

where, W_n represents either W_{ext} or W_{tot} of segment n, and W_{ref} represents the reference value of W_{ext} or W_{tot}.

2.4. Simulation set-up

Electrical remodeling was simulated using a cardiac fiber with a reference length of 1 cm. With stimulation

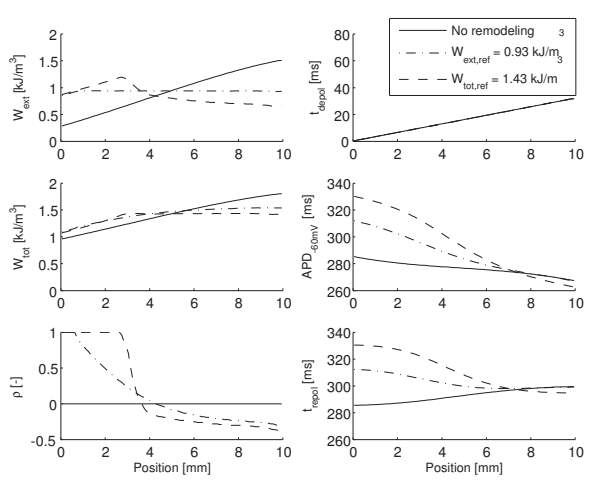

Figure 2. Effect of electrical remodeling of $I_{\mathrm{Ca,L}}$ on the cardiac fiber. Left: external stroke work density (W_{ext}), total stroke work density (W_{tot}), and parameter ρ. Right: time of depolarization (t_{depol}), action potential duration ($\mathrm{APD}_{-60\mathrm{mV}}$), and time of repolarization (t_{repol}). Solid line: no remodeling. Dash-dotted line: remodeling controlled by W_{ext}. Dashed line: remodeling controlled by W_{tot}. A stimulus current was applied to the first segment at 0 ms.

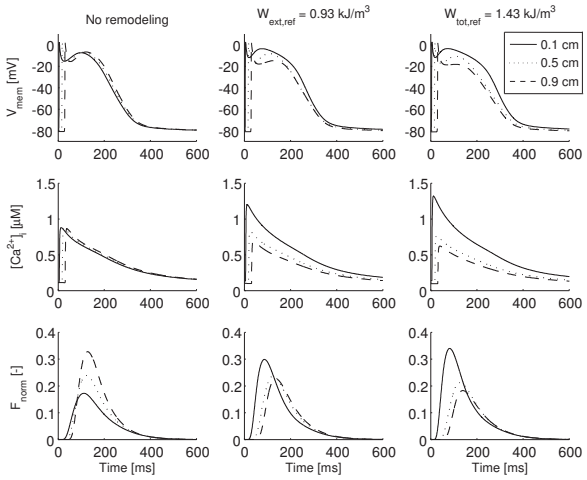

Figure 3. Effect of electrical remodeling of $I_{\mathrm{Ca,L}}$ on individual segments. Membrane potential (V_{mem}), intracellular Ca^{2+} concentration ($[\mathrm{Ca}^{2+}]_{\mathrm{i}}$), and normalized contractile force (F_{norm}) are plotted for segments located at 0.1, 0.5, and 0.9 cm. Left: without remodeling. Center: remodeling controlled by W_{ext} ($W_{\mathrm{ext,ref}} = 0.93$ kJ/m^2). Right: remodeling controlled by W_{tot} ($W_{\mathrm{tot,ref}} = 1.43$ kJ/m^2). A stimulus current was applied to the segment at 0.0 cm at 0 ms.

rate 1 Hz, a depolarization wave was generated by electrical stimulation of the first segment. Depolarization of the entire fiber took 32 ms (conduction velocity 0.32 m/s). The cardiac cycle was simulated with $T_{\mathrm{rest}} = 0.5$ kPa, $T_{\mathrm{preload}} = 1$ kPa, and $T_{\mathrm{afterload}} = 10$ kPa. Electrical remodeling was controlled either by W_{ext} ($W_{\mathrm{ext,ref}} = 0.93$ kJ/m^3) or W_{tot} ($W_{\mathrm{tot,ref}} = 1.43$ kJ/m^3). In both cases, a final distribution of the ρ_n was reached in at most 140 cardiac cycles. By simulating 150 cardiac cycles, it was ensured that steady-state was reached.

3. Results

In Figure 2, W_{ext}, W_{tot}, parameter ρ, time of depolarization (t_{depol}), $\mathrm{APD}_{-60\mathrm{mV}}$, and time of repolarization (t_{repol}) are presented for each location along the fiber with and without remodeling. Here, $\mathrm{APD}_{-60\mathrm{mV}} = t_{\mathrm{repol}} - t_{\mathrm{depol}}$ is defined as the time during which V_{mem} is larger than -60 mV. Without remodeling, W_{ext} and W_{tot} are small for early-activated segments and larger for later-activated segments. With remodeling, both W_{ext} and W_{tot} are increased for early-activated segments and decreased for later-activated segments, such that a more homogeneous distribution is obtained. In the case that remodeling is controlled by W_{tot}, the reference value ($W_{\mathrm{tot,ref}} = 1.43$ kJ/m^2) is not reached for early-activated segments, while parameter ρ reaches its maximum value of 1.0. Electrical remodeling has no effect on t_{depol}, i.e., the conduction velocity is not affected. On the other hand, t_{repol} is significantly changed with remodeling due to the increase in $\mathrm{APD}_{-60\mathrm{mV}}$ for early-activated segments and the decrease for later-activated segments. A consequence of these changes is that the repolarization wave is reversed.

In Figure 3, the effect of electrical remodeling on the membrane potential (V_{mem}), intracellular Ca^{2+} concentration ($[\mathrm{Ca}^{2+}]_{\mathrm{i}}$), and the normalized contractile force (F_{norm}) is illustrated for the segments located at 0.1, 0.5, and 0.9 cm. Without remodeling, the APs and Ca^{2+} transients have similar morphology and duration. With remodeling, the AP and Ca^{2+} transient of the segment at 0.1 cm envelops the APs and Ca^{2+} transients of the other two segments. In addition, F_{norm} is increased for the early-activated segment and decreased for the later-activated segment, which is related to the more homogeneous distribution of stroke work (Figure 2).

In Figure 4, the effect of electrical remodeling on stress, strain, and the stress-strain loop is illustrated for the segments located at 0.1, 0.5, and 0.9 cm. With remodeling, shortening increases for early-activated segments and decreases for later-activated segments. The overall effect is a more homogeneous shortening of the fiber during ejection. The more homogeneous distribution of W_{ext} with remodeling is reflected by the fact that the areas enclosed by the stress-strain loops are about the same size with remodeling.

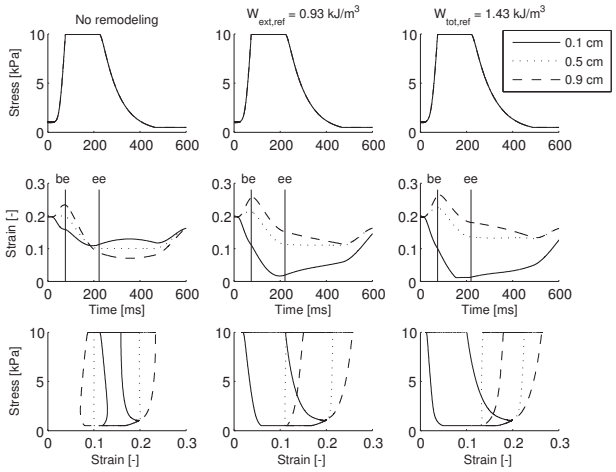

Figure 4. Effect of electrical remodeling of $I_{\mathrm{Ca,L}}$ on the stress-strain loop for individual segments. Stress, strain, and stress-strain loops are plotted for segments located at 0.1, 0.5, and 0.9 cm. Left: without remodeling. Center: remodeling controlled by W_{ext} ($W_{\mathrm{ext,ref}} = 0.93$ kJ/m^2). Right: remodeling controlled by W_{tot} ($W_{\mathrm{tot,ref}} = 1.43$ kJ/m^2). A stimulus current was applied to the segment at 0 ms. Begin and end of ejection are indicated with be and ee, respectively.

4. Discussion and conclusions

With homogeneous electrophysiology, stroke work was small in early-activated segments and large in later-activated segments. By adapting $I_{\mathrm{Ca,L}}$ to homogenize stroke work, a more homogeneous muscle contraction was obtained. In addition, AP duration was increased in early-activated and decreased in later-activated segments, which lead to a reversed repolarization wave. These results are in agreement with experimental observations in animals with long-term asynchronous activation [3, 12]. Our findings suggest that the abnormal electromechanics in paced ventricles leads to adaptation through mechanoelectric feedback. An effect of this adaptation is the reversal of the repolarization wave, which affects the T wave in the ECG and is consistent with experimental findings [4]. In addition, the large regional differences in mechanical workload are somewhat reduced.

In conclusion, adaptive modeling of electrophysiology may lead to better predictions of cardiac electrophysiology and mechanics in coupled models of cardiac electromechanics. As the Ca^{2+} transient and the plateau phase of the AP are determined by a balance between the depolarizing $I_{\mathrm{Ca,L}}$ and the repolarizing K^+ currents, a possible improvement of our model is to take the effect of electrical remodeling of the K^+ currents into account.

References

[1] Cordeiro JM, Greene L, Heilmann C, Antzelevitch D, Antzelevitch C. Transmural heterogeneity of calcium activity and mechanical function in the canine left ventricle. Am J Physiol Heart Circ Physiol 2004;286:H1471–H1479.

[2] Kerckhoffs RCP, Bovendeerd PHM, Kotte JCS, Prinzen FW, Smits K, Arts T. Homogeneity of cardiac contraction despite physiological asynchrony of depolarization: a model study. Ann Biomed Eng 2003;31:536–547.

[3] Prinzen FW, Hunter WC, Wyman BT, McVeigh ER. Mapping of regional myocardial strain and work during ventricular pacing: experimental study using magnetic resonance imaging tagging. J Am Coll Cardiol 1999;33:1735–1742.

[4] Rosenbaum MB, Blanco HH, Elizari MV, Lazzari JO, Davidenko JM. Electrotonic modulation of the T wave and cardiac memory. Am J Cardiol 1982;50:213–222.

[5] Jeyaraj D, Wilson LD, Zhong J, Flask C, Saffitz JE, Deschênes I, Yu X, Rosenbaum DS. Mechanoelectric feedback as novel mechanism of cardiac electrical remodeling. Circulation 2007;115:3145–3155.

[6] Sosunov EA, Anyukhovsky EP, Rosen MR. Altered ventricular stretch contributes to initiation of cardiac memory. Heart Rhythm 2008;5:106–113.

[7] Kuijpers NHL, ten Eikelder HMM, Bovendeerd PHM, Verheule S, Arts T, Hilbers PAJ. Mechanoelectric feedback leads to conduction slowing and block in acutely dilated atria: a modeling study of cardiac electromechanics. Am J Physiol Heart Circ Physiol 2007;292:H2832–H2853.

[8] Kuijpers NHL, Rijken RJ, ten Eikelder HMM, Hilbers PAJ. Vulnerability to atrial fibrillation under stretch can be explained by stretch-activated channels. Comput Cardiol 2007;34:237–240.

[9] Kuijpers NHL, ten Eikelder HMM, Bovendeerd PHM, Verheule S, Arts T, Hilbers PAJ. Mechanoelectric feedback as a trigger mechanism for cardiac electrical remodeling: a model study. Ann Biomed Eng 2008; *in press*.

[10] Courtemanche M, Ramirez RJ, Nattel S. Ionic mechanisms underlying human atrial action potential properties: insights from a mathematical model. Am J Physiol Heart Circ Physiol 1998;275:H301–H321.

[11] Rice JJ, Winslow RL, Hunter WC. Comparison of putative cooperative mechanisms in cardiac muscle: length dependence and dynamic responses. Am J Physiol Heart Circ Physiol 1999;276:H1734–H1754.

[12] Plotnikov AN, Yu H, Geller JC, Gainullin RZ, Chandra P, Patberg KW, Friezema S, Danilo Jr P, Cohen IS, Feinmark SJ, Rosen MR. Role of L-type calcium channels in pacing-induced short-term and long-term cardiac memory in canine heart. Circulation 2003;107:2844–2849.

Address for correspondence:

Nico Kuijpers
Department of Biomedical Engineering (CARIM)
Maastricht University
P.O. Box 616, 6200 MD Maastricht
The Netherlands
E-mail: nico.kuijpers@bf.unimaas.nl